Colloidal ZnSe, ZnSe/ZnS, and ZnSe/ZnSeS Quantum Dots Synthesized from ZnO

Hsueh-Shih Chen,* Bertrand Lo, Jen-Yu Hwang, Gwo-Yang Chang, Chien-Ming Chen, Shih-Jung Tasi, and Shian-Jy Jassy Wang

Union Chemical Laboratories, Industrial Technology Research Institute, 321, Kuang Fu Rd. Sec.2, Hsin Chu, Taiwan 300, R.O.C.

Received: July 6, 2004; In Final Form: August 12, 2004

Colloidal ZnSe quantum dots were successfully synthesized from ZnO in a lauric acid/hexadecylamine mixture. X-ray diffraction patterns indicated that the ZnSe quantum dots possess a wurtzite structure. Transmission electron microscope images of the quantum dots showed that the average diameter are in the range of 25∼60 Å. The size-dependent photoluminescence was controlled from 400 to 440 nm with the quantum yields of 6∼10% at room temperature. After passivation with 1.8 monolayer of ZnS overcoat by a traditional two-step method, the quantum yields of ZnSe/ZnS QDs are increased ∼4.5-fold (quantum yield ∼32%). An in-situ method of overcoating was done by directly injecting TOPS into the flask containing ZnSe, ZnO/lauric acid/hexadecylamine, and TOPSe. The photoluminescence quantum yields were improved ∼3.8-fold after introduction of 1.6 monolayer ZnSeS overcoat to the ZnSe QDs.

Introduction

Semiconductive colloidal quantum dots (QDs) that exhibit quantum confinement effect (QCE) have drawn significant attention over the past decade.[1−6] Among III−V and II−VI semiconductive QDs, colloidal CdSe QDs have been examined mostly because of their high emission efficiency and size-tuned photoluminescence (PL).[7−13] However, the band gap of bulk CdSe is 1.74 eV (∼712 nm) and is difficult to be tuned to UV range. Recently, the wide band gap materials have been studied to develop UV emission materials.[14−19] ZnSe is a typical material used for UV−blue light emitting or laser diodes.[20] Colloidal ZnSe QDs using organometallic diethylzinc as a precursor has been first proposed by Hines et al.[17] These QDs exhibited strong luminescence and sized-tuned color in the UV−blue range. However, the diethylzinc (Et_2Zn) is expensive and also toxic like dimethylcadmium that is being replaced by CdO to prepare CdSe QDs.[21]

This article reports the synthesis of ZnSe QDs using ZnO as a precursor, overcoating of the ZnS shell using the conventional two-step method, and in-situ overcoating of ZnSeS in a single step.

Experimental Section

In a typical synthesis of colloidal ZnSe QDs, the Zn precursor was prepared by dissolving 5 mmol of ZnO (99.9%) in a mixture of 25 mmol lauric acid (LA, 99%) and 8 mmol hexadecylamine (HDA, 95%) at ∼300 °C under argon flow. The Se precursor was prepared by dissolving 5 mmol of Se powder in 6.5 mmol of trioctylphosphine (TOP, 90%). After cold Se precursor was injected into the hot Zn precursor, ZnSe nuclei formed and the temperature dropped to ∼280 °C. The reduction of temperature stops the nucleation but allows the nuclei to continue growing. The ZnSe nanocrystal sizes were controlled by different growth time. The product was washed by hot methanol and collected by a size-selective method.[2]

Typical two-step passivation shell growth of QDs employs dangerous organometallic compounds such as diethylzinc in TOPO or TOP at ∼160 °C as precursors.[7,22−24] Reiss et al. proposed an alternative shell precursor that uses zinc stearate or ZnO/dodecylphosphonic acid complex along with TOPSe to grow ZnSe shell on CdSe core.[25] In their experiments, the injection temperature of ZnO/dodecylphosphonic acid complex was higher than that of zinc stearate (≥200 °C).

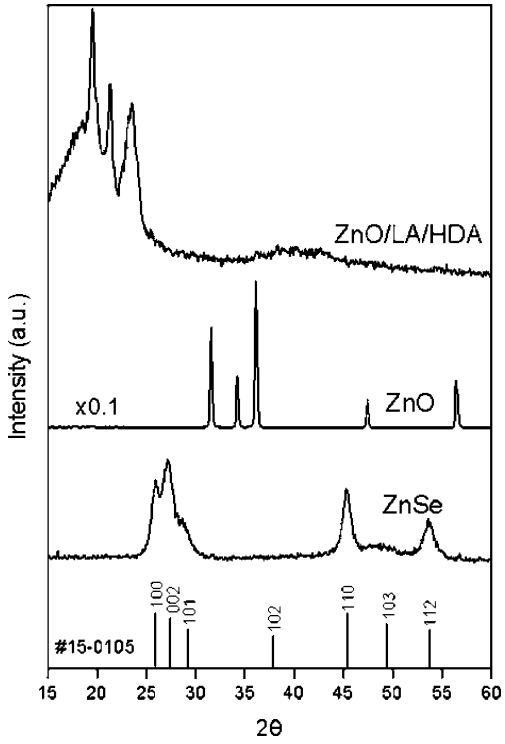

Figure 1. XRD patterns of ZnO/LA/HDA complex, ZnO, and ZnSe QDs. The peaks were indexed as wurtzite ZnSe nanocrystals.

In our experiments, conventional two-step overcoat growth and in-situ overcoat growth approaches were performed. For the traditional two-step overcoating process, the bare ZnSe cores were initially prepared and dispersed into LA/HDA mixture. The Zn precursor used was prepared by dissolving 3 mmol ZnO in LA/HDA (15 mmol/4.8 mmol) at 300 °C and then cooling to ∼80 °C. The sulfur stock solution, TOPS, was prepared by

* Corresponding author. E-mail: sean@itri.org.tw.

10.1021/jp047035w CCC: $27.50
Published on Web 10/08/2004

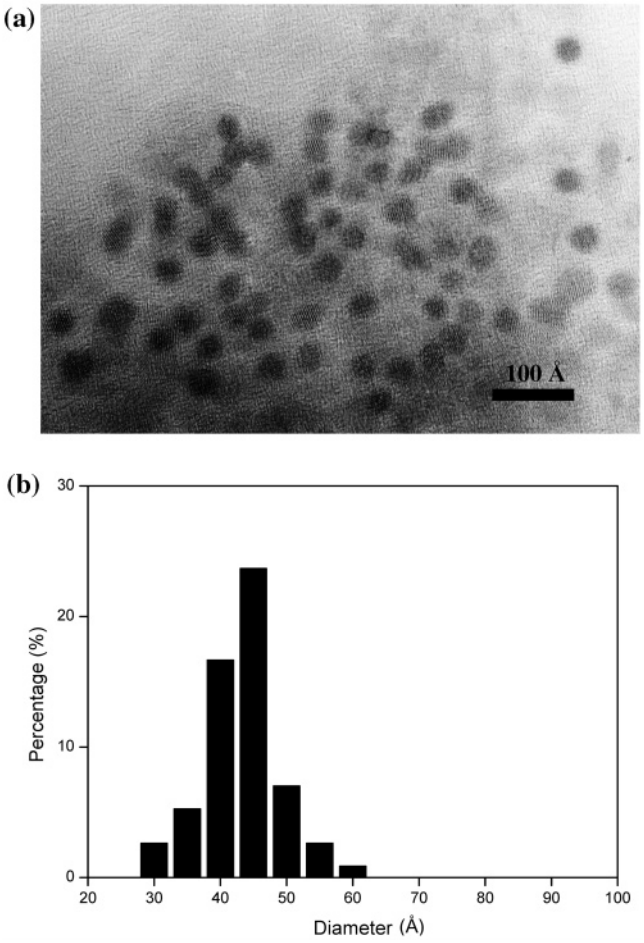

Figure 2. (a) HRTEM image of ZnSe QDs grown for 18 min. (b) Size histograms of specimens estimating the longest dimension for over 100 particles. The mean diameter was 45 Å ± 15%.

dissolving 3 mmol S in 22 mmol TOP. The ZnO/LA/HDA and TOPS mixture was injected into the LA/HDA containing 100 mg ZnSe cores at 180 °C. The injection rate was kept at ~0.1 mL/min.

For the in-situ ZnSeS overcoating process, the TOPS solution was directly injected into the flask while the growth of ZnSe QDs was taking place. The ZnSe cores were first prepared as in the two-step process (ZnO/Se/LA/HDA/TOP = 6 mmol/5 mmol/25 mmol/8 mmol/6.5 mmol). The TOPS stock solution was prepared by dissolving 3 mmol S in 22 mmol TOP. At the appropriate time, the TOPS solution was injected into the flask containing growing ZnSe cores, Zn monomer, and Se monomer. In this synthesis, the TOPS, Zn monomer, and Se monomer acted as overcoat precursors. The ZnSeS overcoat thickness was controlled by varying the ZnSeS growth time.

The specimens were analyzed using X-ray diffractometer (XRD, XD-D1 Shimadzu), high-resolution transmission electron microscope (HRTEM, JEOL JEM-4000EX), photoluminescence spectrophotometer (PL, Hitachi F-4500 Fluorescence Spectrophotometer), and UV/vis spectrophotometer (Hitachi U-2010 UV/Vis Spectrophotometer). The elemental compositions of the specimens were analyzed using energy-dispersive X-ray spectrometry (EDS, Oxford ISIS X-ray EDS microanalysis system attached to the TEM).

The PL quantum yield (QY) of ZnSe QDs in toluene was estimated relative to Stilbene 420 in methanol of the same optical absorbance (~0.01) under 350-nm excitation.

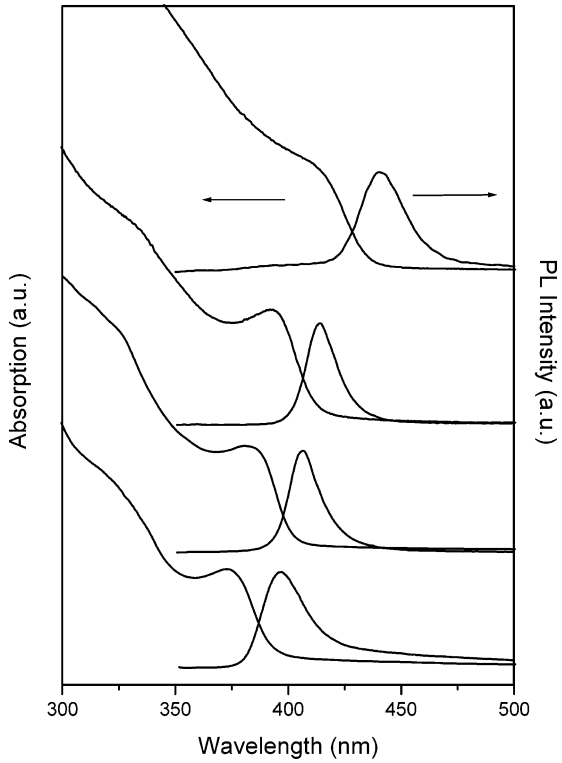

Figure 3. Room-temperature PL and optical absorption spectra of ZnSe QDs dispersed in toluene. The growth time of ZnSe QDs were 5 (29 Å), 10 (32 Å), 18 (45 Å), and 40 min (58 Å). The QYs were 8.5, 7.8, 7.2, and 6.2% for 29, 32, 45, and 58 Å ZnSe QDs, respectively. The particle sizes were estimated using TEM analyses. The excitation wavelength is 350 nm.

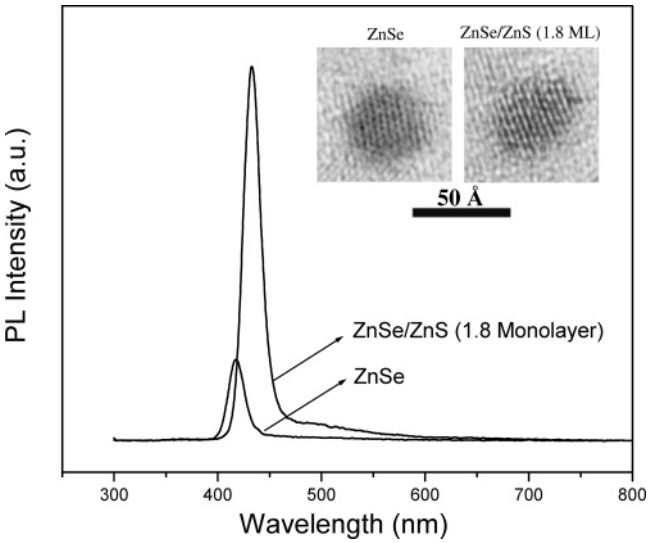

Figure 4. PL spectra from ZnSe and ZnSe/ZnS QDs. The PL intensity of the ZnSe/ZnS QDs was enhanced by a factor ~4.5 after coating with ZnS. The QYs of ZnSe and ZnSe/ZnS QDs were 7.2 and 32.4%, respectively. The inset is HRTEM images of ZnSe before and after coating with 1.8 monolayer ZnS shell.

Results and Discussion

The ZnO is amphoteric and dissolves both in acids and alkalis. Zn tends to form complexes with ligands containing O-, N-, or S-donor atoms. Because of the filled d shell of Zn, there is no crystal field to be considered in the metal−ligand complex, and the stereochemistry of this metal−ligand complex is determined by size and polarizing power of the metal ion. Since the Zn ion is small, short-chain-length ligands are considered suitable for

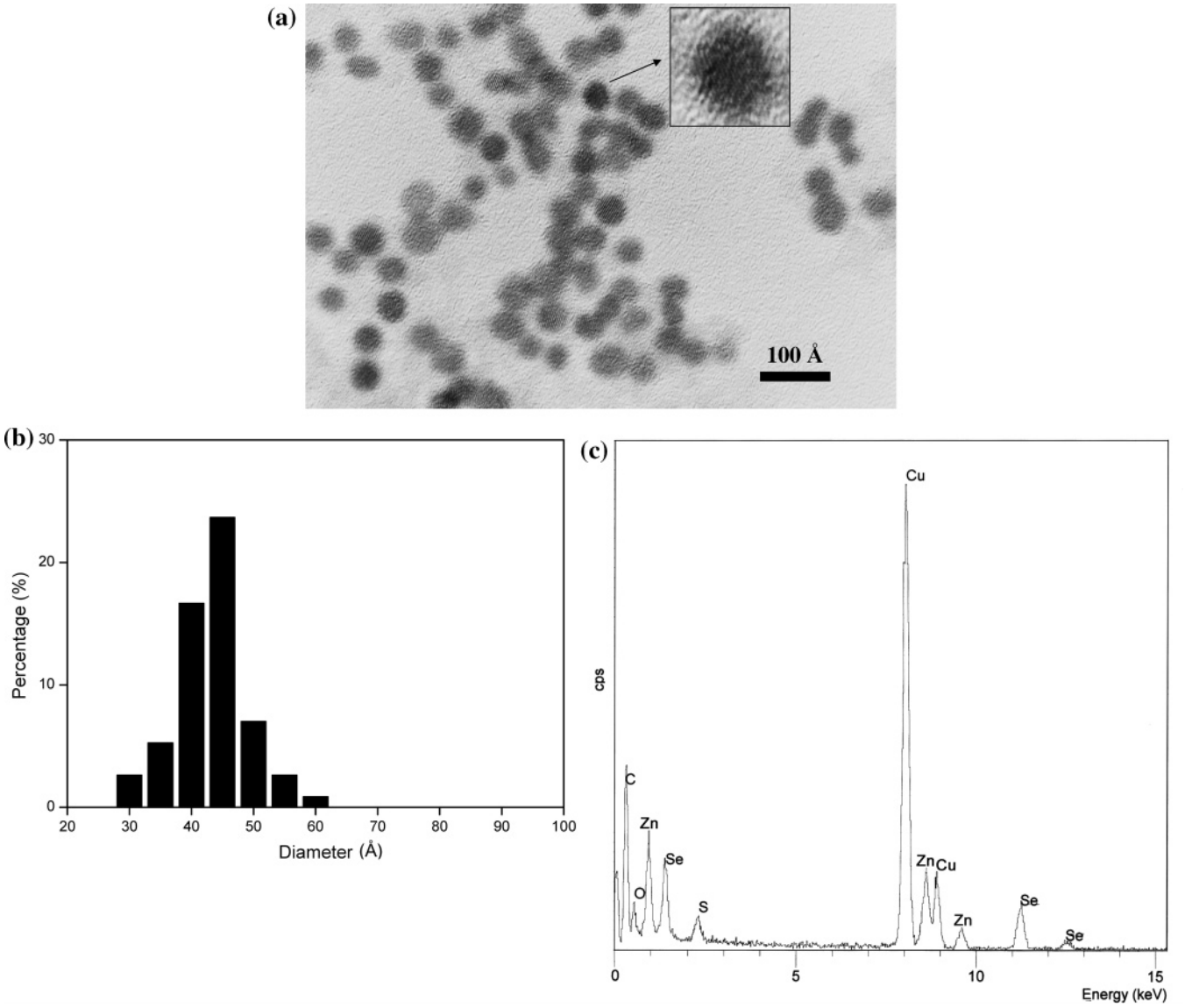

Figure 5. (a) HRTEM image of in-situ ZnSeS-overcoated ZnSe QDs. TOPS was injected into the flask at 18 min and allowed to react for 6 more minutes. (b) Size histograms of specimens. The mean diameter was 48 Å ± 13%. (c) EDS spectrum of the specimen. The appearance of Zn, Se, and S signals indicates the overcoat is ZnSeS alloy.

synthesis. The smaller coordinating ligands can better cover Zn ions. Thus, LA was used to dissolve ZnO by forming a complex. Theoretically, a 1:2 ratio of Zn to LA is sufficient to coordinate all Zn atoms. However, ZnO cannot dissolve completely when the ratio of LA to Zn is smaller than three. This may be due to evaporation or degradation of LA at high temperatures or to the coordination reaction rate being extremely slow.

The Zn/LA complex degraded at higher temperature (~220 °C). An elevated reaction temperature (generally, >250 °C) is needed to form high crystalline colloidal QDs. The cosolvent HDA was served as a coordinating surfactant in the synthesis. The HDA not only raised the reaction temperature but also narrowed the size distribution of ZnSe QDs similar to CdSe QDs.[26,27] In the case of ZnO with LA/HDA, controlled growth of ZnSe QDs was fairly successful.

The solvent and cosolvent are coordinating surfactants, affecting both the nucleation and the growth stages. Accordingly, the coordinating solvents with suitable chain lengths should be considered. Long-chain length may affect the nucleation and growth of nanocrystals since the chains will block monomer migration. Monomer stability is another factor. Peng and Peng showed that monomer stability affects the nucleation stage.[28] The boiling temperature of the solvent or cosolvent is also crucial as low temperature will lead to imperfect nanocrystals.

The absence of ZnO peaks in the XRD pattern indicates that the ZnO dissolved completely in the LA/HDA mixture, as shown in Figure 1. The nucleation/growth mechanism was similar to that of CdSe QDs. The rapid injection of TOPSe into the hot ZnO/LA/HDA complex produced numerous ZnSe nuclei, and the nucleation stage was terminated by the sudden temperature fall as soon as TOPSe injected. Instead of nucleation stage, the nanocrystals grew up in a dynamic adsorption−desorption process of the coordinating surfactants on their surface. Eventually, a yellowish product began appearing in the mixture. The diffraction peaks of the product indicated a wurtzite structure for the ZnSe nanocrystals.

Figure 2a shows an HRTEM image of ZnSe QDs dispersed in a copper grid. As shown in the picture, the QDs have well-resolved lattice images, which imply good crystallinity. A size distribution histogram is shown in Figure 2b. The mean diameter of the ZnSe QDs was estimated to be 45 Å ± 15%.

The PL from ZnSe QD sampling at various growth times in Figure 3 shows a narrow peak that was tunable from 400~440 nm. The broader band gaps of these ZnSe QDs, as compared

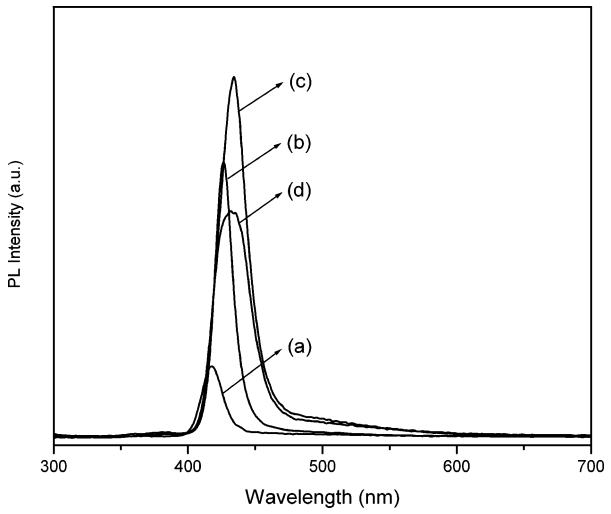

Figure 6. PL of ZnSe/ZnSeS QDs. Sampling at 0, 3, 6, and 9 min after injecting TOPS. (a) Bare ZnSe with QY ~ 6.8%. (b) 0.7 monolayer ZnSeS with QY ~ 22.4% (ZnSeS growth time = 3 min). (c) 1.6 monolayer ZnSeS with QY ~ 26.1% (ZnSeS growth time = 6 min). (d) 2.5 monolayer ZnSeS with QY ~ 14.3% (ZnSeS growth time = 9 min).

to those of bulk ZnSe (2.7 eV, ~459 nm), is ascribed to QCE. The first ZnSe exciton transition peaks were displayed in the optical absorption spectra. The QYs of the ZnSe QDs were between 6 and 10% relative to stilbene 420.

Nonradiative surface dangling bonds or defects of QDs quench PL intensity. Passivation with ZnS has been used to reduce the nonradiative centers on the QD surfaces.[24] Figure 4 depicts PL of the ZnSe and ZnSe/ZnS QDs grown using a conventional two-step approach similar to that of CdSe/ZnSe.[7] The PL intensity of bare ZnSe QDs was improved ~4.5-fold by introduction of 1.8 monolayer of ZnS (QY ~ 32.4%).

For the in-situ ZnSeS overcoating, the Zn and Se monomers were directly used as shell precursors. After injecting TOPS into the hot mixture containing the ZnSe cores, Zn monomer, and Se monomer, the ZnSeS alloy heterogeneously nucleated on the ZnSe cores. ZnSeS shell thickness was varied with growth time. Figure 5a shows HRTEM pictures of ZnSeS-overcoated ZnSe. The mean diameter increased from 45 to 48 Å after the TOPS was injected, as shown in Figure 5b. This implies that the shell overcoated onto the ZnSe nanocrystals. The EDS spectrum reveals the presence of Zn, Se, and S in the specimen, implying that the shells were an alloy of ZnSeS, as shown in Figure 5c.

The PL spectra of ZnSe/ZnSeS QDs displayed enhanced emission intensity after overcoating with ZnSeS, as shown in Figure 6. The PL efficiency of ZnSe QDs was enhanced ~3.7-fold after overcoating with 1.6 monolayer ZnSeS (~26.1%). However, when the ZnSeS overcoating thickness was ~2.5 monolayer, the PL peak broadened and intensity decreased to ~14.3%.

Core/shell interface is not visible in the HRTEM images of both ZnSe/ZnS and ZnSe/ZnSeS QDs. This is presumably due to thin shell coatings on bare ZnSe cores. In fact, the crystal lattice image is the phase contrast contributed by the interference of transmitted and diffracted electron beams. The imaging is significantly affected by the crystal thickness, lattice twist, and defocusing of the electron beam. For ball-like nanocrystals, differences in thickness between the ball centers and ball edges and lattice twists near their surface might affect the formation of the lattice image. Therefore, it is difficult to distinguish the thin ZnSe or ZnSeS shell of the QDs in the TEM images.

The size distribution of ZnSe/ZnSeS QDs was narrower than that of ZnSe QDs. This phenomenon is attributed to the size-focusing effect of the second round of TOPS injection. The carrier confinement of wide band gap ZnS should be more efficient than that of ZnSeS alloy. So, the PL enhancement of ZnSe/ZnS QDs was slightly larger than that of ZnSe/ZnSeS QDs. Although the ZnSeS composite shell confined the carriers to a lesser extent, the in-situ shell overcoats simplified the shell passivation process in comparison with the conventional two-step approach. We have also demonstrated that in-situ CdZnSe overcoating of bare CdSe cores improved PL intensity 4~6-fold.

Conclusion

In summary, colloidal ZnSe QDs were successfully synthesized from ZnO powder. Size-tuned band gap was achieved by a growth control process for the ZnSe QDs. The QDs showed controlled PL emission from 400 to 440 nm with quantum yields from 6 to 10% at room temperature. By passivating 1.8 monolayer of ZnS overcoat onto bare ZnSe using the conventional two-step method, the PL QY of ZnSe/ZnS QDs increased ~4.5-fold, whereas ZnSe/ZnSeS PL QY was improved ~3.8-fold after introduction of 1.6 monolayer composite ZnSeS overcoating onto bare ZnSe cores using the in-situ ZnSeS overcoating process. The results show a potential for preparation of colloidal ZnSe, ZnSe/ZnS, and ZnSe/ZnSeS QDs from cheap and nontoxic ZnO.

Acknowledgment. The authors would like to thank the Industrial Technology Research Institute of the R.O.C., Taiwan for financially supporting this research under contract No. A331XS3N10.

References and Notes

(1) Bawendi, M. G.; Wilson, W. L.; Rothberg, L.; Carroll, P. J.; Jedju, T. M.; Steigerwald, M. L.; Brus, L. E. *Phys. Rev. Lett.* **1990**, *65*, 1623.
(2) Murray, C. B.; Norris, D. J.; Bawendi, M. G. *J. Am. Chem. Soc.* **1993**, *115*, 8706.
(3) Guzelian, A. A.; Banin, U.; Kadavanich, A. V.; Peng, X.; Alivisatos, A. P. *Appl. Phys. Lett.* **1996**, *69*, 1432.
(4) Alivisatos, A. P. *Science* **1996**, *271*, 933.
(5) Wu, Q.; Zheng, N.; Li, Y.; Ding, Y. *J. Membr. Sci.* **2000**, *172*, 199.
(6) Chen, S.; Liu, W. *Langmuir* **1999**, *15*, 8100.
(7) Danek, M.; Jensen, K. F.; Murray, C. B.; Bawendi, M. G. *Chem. Mater.* **1996**, *8*, 173.
(8) Rodriguez-Viejo, J.; Jensen, K. F.; Mattoussi, H.; Michel, J.; Dabbousi, B. O.; Bawendi, M. G. *Appl. Phys. Lett.* **1997**, *70*, 2132.
(9) Peng, X.; Schlamp, M. C.; Kadavanich, A. V.; Alivisatos, A. P. *J. Am. Chem. Soc.* **1997**, *119*, 7019.
(10) Hines, M. A.; Guyot-Sionnest P. *J. Phys. Chem. B* **1996**, *100*, 468.
(11) Peng, X.; Manna, L.; Yang, W.; Wickham, J.; Scher, E.; Kadavanich, A.; Alivisatos, A. P. *Nature* **2000**, *404*, 59.
(12) Manna, L.; Scher, E. C.; Alivisatos, A. P. *J. Am. Chem. Soc.* **2000**, *122*, 12700.
(13) Bruchez, M., Jr.; Moronne, M.; Gin, P.; Weiss, S.; Alivisatos, A. P. *Science* **1998**, *281*, 2013.
(14) Petersson, A.; Gustafsson, A.; Samuelson, L.; Tanaka, S.; Aoyagi, Y. *Appl. Phys. Lett.* **1999**, *74*, 73513.
(15) Doneg, C. M.; Bol, A. A.; Meijerink, A. *J. Lumin.* **2002**, *96*, 87.
(16) Bhaskar, S.; Dobal, P. S.; Rai, B. K.; Katiyara, R. S. *J. Appl. Phys.* **1999**, *85*, 439.
(17) Hines, M. A.; Guyot-Sionnest P. *J. Phys. Chem. B* **1998**, *102*, 3655.
(18) Suyver, J. F.; Wuister, S. F.; Kelly, J. J.; Meijerink, A. *Phys. Chem. Chem. Phys.* **2000**, *2*, 5445.
(19) Norris, D. J.; Yao, N.; Charnock, F. T.; Kennedy, T. A. *Nano Lett.* **2001**, *1*, 3.
(20) Bonard, J. M.; Ganiere, J. D.; Vanzetti, L.; Paggel, J. J.; Sorba, L.; Franciosi, A.; Herve D.; Molva, E. *J. Appl. Phys.* **1998**, *84*, 1263.
(21) Peng, Z. A.; Peng, X. *J. Am. Chem. Soc.* **2001**, *123*, 183.

(22) Dabbousi, B. O.; Rodriguez-Viejo, J.; Mikulec, F. V.; Heine, J. R.; Mattoussi, H.; Ober, R.; Jensen, K. F.; Bawendi, M. G. *J. Phys. Chem. B* **1997**, *101*, 9463.
(23) Manna, L.; Scher, E. C.; Li, L.; Alivisatos, A. P. *J. Am. Chem. Soc.* **2002**, *124*, 7136.
(24) Lomascolo, M.; Creti, A.; Leo, G.; Vasanelli, L.; Manna, L. *Appl. Phys. Lett.* **2003**, *82*, 418.
(25) Reiss, P.; Bleuse, J.; Pron, A. *Nano Lett.* **2002**, *2*, 781.
(26) Talapin, D. V.; Rogach, A. L.; Kornowski, A.; Haase, M.; Weller, H. *Nano Lett.* **2001**, *1*, 207.
(27) Reiss, P.; Bleuse, J.; Pron, A. *Nano Lett.* **2002**, *2*, 781.
(28) Peng, Z. A.; Peng, X. *J. Am. Chem. Soc.* **2002**, *124*, 3343.
(29) Xue, J.; Ye, Y.; Medina, F.; Martinez, L.; Lopez-Rivera, S. A.; Giriat, W. *J. Lumin.* **1998**, *78*, 173.